

FullTransNet: Full Transformer with Local-Global Attention for Video Summarization

Libin Lan^{ib}, *Member, IEEE*, Lu Jiang^{ib}, Tianshu Yu^{ib}, Xiaojuan Liu^{ib}, and Zhongshi He^{ib}

Abstract—Video summarization mainly aims to produce a compact, short, informative, and representative synopsis of raw videos, which is of great importance for browsing, analyzing, and understanding video content. Dominant video summarization approaches are generally based on recurrent or convolutional neural networks, even recent encoder-only transformers. We propose using full transformer as an alternative architecture to perform video summarization. The full transformer with an encoder-decoder structure, specifically designed for handling sequence transduction problems, is naturally suitable for video summarization tasks. This work considers supervised video summarization and casts it as a sequence-to-sequence learning problem. Our key idea is to directly apply the full transformer to the video summarization task, which is intuitively sound and effective. Also, considering the efficiency problem, we replace full attention with the combination of local and global sparse attention, which enables modeling long-range dependencies while reducing computational costs. Based on this, we propose a transformer-like architecture, named FullTransNet, which has a full encoder-decoder structure with local-global sparse attention for video summarization. Specifically, both the encoder and decoder in FullTransNet are stacked the same way as ones in the vanilla transformer, and the local-global sparse attention is used only at the encoder side. Extensive experiments on two public multimedia benchmark datasets SumMe and TVSum demonstrate that our proposed model can outperform other video summarization approaches, achieving F-Measures of 54.4% on SumMe and 63.9% on TVSum with relatively lower compute and memory requirements, verifying its effectiveness and efficiency. The code and models are publicly available on [GitHub](#).

Index Terms—FullTransNet, sparse attention, transformer, video summarization.

I. INTRODUCTION

WITH the popularity of various devices for video capturing, watching, and storage, coupled with the widespread use of video-sharing platforms (e.g., YouTube) and social media networks (e.g., Facebook), The amount of

video data is increasing at an unprecedented rate. This makes it challenging to efficiently browse and find relevant content [1], [2], [3]. To tackle the challenging problem, automatic and efficient video summarization techniques are increasingly needed. Video summarization essentially condenses a video by selecting the most informative parts to create a summary that represents the original content. The created summary can either be a static video storyboard, consisting of a set of representative keyframes, or a dynamic video skim made up of key shots [4]. In our work, we focus on creating summaries based on key shots for three main reasons. First, viewers are more interested in watching video skims than static storyboards. Second, key shots contain diverse information and can highly represent source video. Last but not least, in practice, a video is usually segmented into continuous and non-overlapping shots, which retain intrinsic visual-temporal coherence. These advantages ensure the selected segments effectively reflect the overall theme and storyline of the video, which can yield a comfortable and entertaining user experience, even if it accounts for only a small percentage of the whole content [3], [5], [6], [7], [8], [9]. In addition, considering the challenges and inherent characteristics of general video summarization tasks, it is of great significance to study general single video summarization techniques for the whole video summarization community [10]. Thus, our special focus is put on the single video summarization technique, without introducing additional correlated signals or domain knowledge from multiple or domain-specific videos, such as VJMHT [11] for co-summarization, TopicSum [12], and HMT [13] for multimodal video summarization, to improve the ability of the summarization model.

Up to now, numerous impactive single video summarization techniques have been proposed and made significant success. These techniques include, but are not limited to, clustering-based [14], change-detection-based [15], dictionary-based [16], and user-attention-based [17], which belong to the scope of conventional non-learning methods, as well as convolutional neural network (CNN)-based [18], recurrent neural network (RNN)-based [4], [5], [6], [19], [20], graph convolutional network (GCN)-based [8], [21], [22], transformer-based (but only encoder architecture) [23], and attention mechanism-based [3], [24], [25], [26], [27], which fall in the field of deep learning methods. Currently, an increasing number of approaches have adopted advanced deep neural network architectures, such as CNN, RNN, even GCN, and encoder-only transformer, for video summarization, and many empirical results show that their performance outperforms that of traditional methods in most cases [4], [8], [23]. This is be-

This paragraph of the first footnote will contain the date on which you submitted your paper for review. This work was supported in part by the Scientific Research Foundation of Chongqing University of Technology under Grants 0103210650 and 0121230235, and in part by the Youth Project of Science and Technology Research Program of Chongqing Education Commission of China under Grants KJQN202301145 and KJQN202301162. (*Corresponding authors: Libin Lan.*)

Libin Lan and Lu Jiang are with the College of Computer Science and Engineering, Chongqing University of Technology, Chongqing 400054, China (e-mail: lanlbn@cqu.edu.cn; bdml_jl@stu.cqu.edu.cn).

Tianshu Yu is with the School of Data Science, Chinese University of Hong Kong, Shenzhen 518172, China (e-mail: yutianshu@cuhk.edu.cn).

Xiaojuan Liu is with the College of Artificial Intelligence, Chongqing University of Technology, Chongqing 401135, China (e-mail: liuxiaojuan0127@cqu.edu.cn).

Zhongshi He is with the College of Computer Science, Chongqing University, Chongqing 400044, China (e-mail: zshe@cqu.edu.cn).

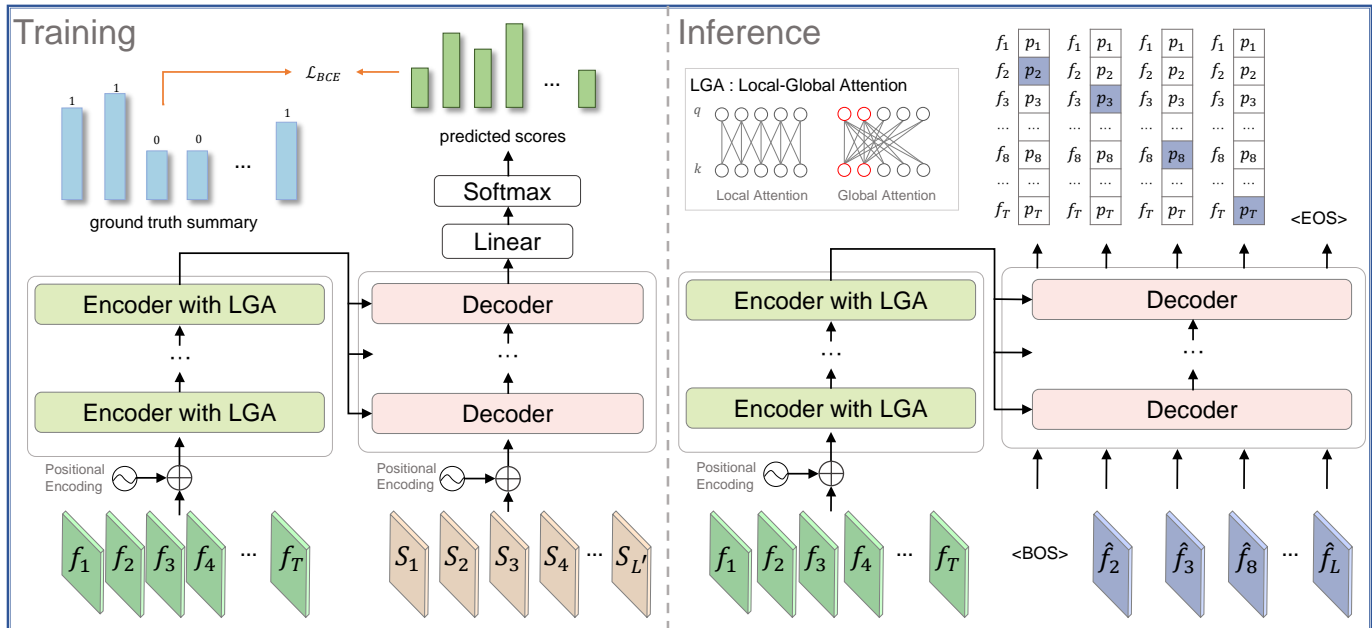


Fig. 1. Motivation and Main Idea. Our core idea is to directly apply full transformer architecture to video summarization and to substitute local-global attention for full attention. Our main aim is to perform video summarization in an end-to-end manner and to save computational cost without sacrificing performance. This illustration demonstrates how to implement our idea and achieve our purpose from the two processes of training and inference. Symbols f , s , \hat{f} , T , L' and L represent frame in original video, keyshot in summary, predicted keyframe, the number of frames in original video, the number of shots in summary, and the number of frames in summary, respectively.

cause CNN and RNN have a powerful ability to extract frame spatial information and model temporal correlations between frames, respectively. In addition, compared to unsupervised learning approaches, supervised learning approaches in general can achieve better performance [4], [19]. This is because supervised signals from ground truth can be more beneficial for model training. Thus, this work considers supervised video summarization and adopts deep models as our single video summarization techniques.

Although CNN and RNN have dominated the video summarization task, CNN has limitations in modeling global dependencies, which is because convolutional operations only rely on a deep stack of multiple convolutional layers to capture long-range dependencies, while RNN has no parallelism inherently since it uses recursive structures to model long-range dependencies in which current input depends on previous output. Different from CNN and RNN, transformer [28] utilizes self-attention mechanism to capture long-range dependencies among tokens and to support more parallelization computation. Furthermore, the transformer naturally excels at processing sequence data, particularly for input sequences of varying lengths in natural language processing tasks [29], [30]. Its superiority has been witnessed in solving sequence-to-sequence (seq2seq) problems [31], [32], [33]. Since we treat video summarization as a seq2seq learning problem, applying transformer architecture to our video summarization task is intuitively feasible and practical.

Although transformer is an effective tool for seq2seq modeling and has a powerful ability to capture long-range dependencies, it typically suffers from quadratic computational complexity and a heavy memory footprint in terms of sequence

length. Thus, it is necessary to find an efficient way to deal with this problem. In this work, we consider substituting a sparse attention mechanism, termed **Local-Global Attention (LGA)**, which is a combination of local attention and global attention, for vanilla attention in transformer [28]. The main purpose of doing this is to improve efficiency without hurting performance. To this end, in our work local attention is used to learn neighbor tokens concerning one query, while global attention is used to attend to all tokens. According to prior observations and findings in language understanding [34], [35], [36], sparse attention mechanisms can achieve a balance between efficiency and performance. Empirical results on our vision task also support a similar insight, that is, LGA is very helpful for improving the efficiency of vanilla attention.

Considering the aforementioned superiority of both transformer and sparse attention, we attempt to use full transformer (with encoder-decoder structure), called **FullTransNet**, as an alternative resolution to model the seq2seq problem in video summarization. Concretely, the inputs of encoder are source sequences, i.e., frame sequences of original video, while the inputs of decoder are target sequences, i.e., ground-truth sequences of shot-level video summary in training or predicted sequences in inference. **During training**, the encoder encodes the input frame sequences in parallel using self-attention, while the decoder using cross-attention allows each query summary frame to attend to the information of all frames from the encoder, and using masked self-attention allows the query frame at the current position to only attend to all key-value frames up to and including this position. **During inference**, the outputs of decoder are the generated summaries based on the resulting trained FullTransNet. In our work, the aforementioned sparse

attention LGA is used only at the encoder side, which is because the decoder works in an auto-regressive manner, that is, the current position only needs to attend to the previous and current position itself; additionally, the length of summary sequence is smaller than that of input original sequence. Thus, for the decoder, it is more efficient to use full self-attention than sparse attention, while for the encoder, applying LGA can effectively reduce the computational burden as the length of sequences increases. This viewpoint is consistent with one in BigBird [35].

In summary, we use the encoder with sparse attention to compute the representation of the entire video, in which the full self-attention is replaced with local-global sparse attention. This ensures that the proposed model is not only able to learn the most relevant local information but also has the capability of modeling long-range dependencies. The decoder exploits these rich context representations and query summary frame sequences to generate video summaries. **Our motivation and main idea** are illustrated in Fig. 1. Due to the powerful representation ability of full transformer, there is no need to design specific criteria to make proposed method cover all the properties of generated summaries, such as compactness, diversity, representativeness, and informativeness [4], [7], [37]. We train the model in a supervised learning manner, and make the created summaries by the trained model perfectly cater to the annotator's taste. That is, these generated summaries can represent the main content of the video and preserve their inherent semantic coherence.

Quantitative and qualitative evaluations on two public benchmarks: SumMe [1] and TVSum [2] demonstrate the effectiveness of our proposed method. Particularly, visualization of attention maps in encoder, decoder, and encoder-decoder shows well how our FullTransNet works.

Our main contributions are three-fold as follows:

- 1) Our work provides new insights into how to generate more accurate video summaries by using full transformer architecture, which is the first attempt to be applied to video summarization. Compared to the encoder-only architecture, the full transformer architecture can offer an intuitive and comprehensible way for sequence-to-sequence modeling and simultaneously produce promising results.
- 2) We introduce sparse attention instead of full attention into all layers of the encoder, in which the sparse attention is a combination of local and global attention. This idea mainly aims to reduce computational burden without sacrificing performance.
- 3) We conduct extensive experiments on two popular datasets: SumMe and TVSum, demonstrating the potential to use full Transformer structure for video summarization. To the best of our knowledge, it is the first work to attempt to apply the full transformer structure and sparse attention mechanism for video summarization, which can obtain promising results.

The rest of this paper is organized as follows. Section II delves into the findings and empirical evidence derived from prior related works. Section III specifies our method, including the model's architecture and sparse attention mechanism.

Section IV showcases the experimental results and details, particularly, the multi-layer and multi-head visualization of sparse attention mechanism. Section V summarizes our findings and gives the limitations of work and further considerations.

II. RELATED WORK

Our work has connections to deep model- and attention mechanism-based video summarization. Although other machine learning and non-learning algorithms are also typically mainstream solutions, we do not discuss them since our focus is on methods that attempt to apply deep learning techniques, particularly transformer architecture and its attention mechanism, to video summarization tasks.

A. Deep Model Based Video Summarization

1) *Transformer-free Deep Model*: The transformer-free deep model mainly refers to those using CNN or RNN as a crucial building technique. Current dominant sequence transduction architecture, including seq2seq learning [24], [38], structure prediction [4], [26], sequence labeling [18], and subset selection [19], [37], [39], almost all adopt CNN, RNN, or their combinations [4], [5], [6], [18], [20], [40], [41], [42] as building units to design their corresponding models. For this, there are several important reasons. First, the visual feature representations of video frames are typically extracted using pre-trained convolutional neural networks, such as AlexNet [43], GoogLeNet [44], VGGNet [45], and ResNet [46]. Specifically, among these pre-trained networks, GoogLeNet is most commonly used due to its lightweight and efficiency. In our work, for a fair comparison, we also adopt the GoogLeNet pre-trained model to effectively extract visual information from video frames and transform it into certain-dimensional feature vectors. Second, the nature of RNN makes it excel at modeling temporal dependencies among video frames, which thus facilitates an understanding of the temporal dimension of video content. Finally, considering the challenges in modeling the inherent complex spatiotemporal relationships in video, a common approach [40], [41], [42] is to combine CNN and RNN to fully make use of their respective advantages, so as to achieve comprehensive modeling of video content.

Based on the above-mentioned reasons, many techniques using CNN, RNN, or their combinations have been proposed for video summarization. The pioneering work [4] first explores a bidirectional single-layer long short-term memory (LSTM) network for summarizing videos and obtains a desirable result. Due to the limitation that single-layer LSTM can not deal with long videos well, Zhao et al. [5] propose a hierarchical structure, in which the first layer encodes the dependencies among subshots, while the second utilizes bidirectional LSTM to better capture contextual information for selecting key subshots. The promising results encourage Zhao et al. [6] to further make improvements based on the hierarchical structure of video data. To address large feature-to-hidden mapping matrices and long-range temporal dependencies, Zhao et al. [20] propose using a tensor-train embedding layer instead of a hierarchical structure for video summarization. The aforementioned methods all adopt RNN or its variants to

video summarization, without exploring the application of transformers to this task.

On the other hand, some methods propose using CNN for video summarization. Rochan et al. [18] first attempt to explore convolutional networks for video summarization, and propose a fully convolutional sequence model, which increases effective context size by stacks of convolutional operations, thus enabling the network to model long-range dependencies and allowing for limited parallelization. Additionally, some works use the combination of CNN and RNN for video summarization. The key idea of this line of studies is to consider how to model the spatiotemporal structure of the video. For example, Elfeki et al. [41] combine CNN and gated recurrent unit (GRU) to generate spatiotemporal feature vectors that are then used to estimate the importance of each frame. Lal et al. [42] present an encoder-decoder architecture with convolutional LSTMs to model the spatiotemporal relationship among the frames. Yuan et al. [40] use a combination of convolution and LSTM to model the spatial and temporal structure of the video. Although these methods using CNN, RNN, or their combinations have made great success in video summarization, there are inherent limitations in parallel computing. Our work considers applying full Transformer architecture [28] to video summarization, in which a well-known property is high parallelism, thus avoiding multiple layers stacked in CNN and sequential dependencies occurring in RNN.

2) *Transformer-based Deep Model*: Transformer is typically used in three ways, namely encoder-only, decoder-only, and full encoder-decoder architecture, which are commonly adopted in understanding, generation, and transduction tasks, respectively [47]. Currently, the published approaches applied transformer to video summarization primarily adopt encoder-only architecture. For example, Hsu et al. [23] propose a spatiotemporal vision transformer for video summarization by taking into account both inter-frame correlation and intra-frame attention. In order to use multi-video information, as well as multimodal information, such as visual, textual, and audio, some works propose using multimodal transformer architecture for video summarization. For instance, Li et al. [11] propose a hierarchical transformer to explicitly model cross-video high-level semantic information used for co-summarization. Zhu et al. [12] propose a multimodal Transformer model for the topic-aware video summarization, in which its core component, i.e., feature learning module, is used to fuse the extracted features by a multimodal transformer encoder and model temporal motion by a temporal modeling encoder, respectively. Zhao et al. [13] also propose a hierarchical multimodal transformer for video summarization based on the natural structure of video, i.e., frame-shot-video, which can capture the dependencies among frame and shots, and summarize the video by exploiting the scene information formed by shots.

In general, using encoder-only architecture needs to independently learn a generic representation from input data and then maps this representation to output, while using full encoder-decoder architecture makes it possible to directly learn the mappings from input to output. Also, inspired by the

success of transformer in transduction tasks, e.g., machine translation [28] and text summarization [32], [33], [35], in this work we consider employing full transformer structure to directly learn the mapping model from raw video sequences to summary sequences in an end-to-end manner.

B. Attention Based video Summarization

1) *Non-Transformer Attention*: Non-transformer attention mechanism usually refers to those in conjunction with deep models, particularly RNN. This type of attention is used to focus on the previous relevant positions by an accumulated vector in the corresponding task, which has not only demonstrated significant advantages in natural language processing (NLP) tasks, such as machine translation [48], [49] and text summarization [50], [51], but also shown promising progress in computer vision tasks like video summarization [3], [24], [26], [52].

As for transduction tasks, considering the need for the model performance, particular architecture, and specific scenarios, some summarization methods adopt customized mechanisms. For instance, Ji et al. [52] use a semantic preserving loss with tailored attention to evaluate the output of the decoder. Casas et al. [26] propose an attention mechanism to model user interest. As for the network with an encoder-decoder structure, this line of attention mechanisms is in general applied to the decoder, i.e., considering the decoder state. For example, Ji et al. [24], [52] attempt to explore attention-based LSTM as a decoder to generate a sequence of importance scores. Apostolidis et al. [3] use context attention vector from the encoder to combine with the output of the previous time step of the decoder to reconstruct the video. The types of attention mechanisms are typically computed in a sequential manner. Different from these attention mechanisms, transformer attention [28], i.e., self-attention, is performed in a parallel fashion.

2) *Transformer Attention*: In this paper we hypothesize that transformer attention is one adopting self-attention [25], [22], [27], [53], [54]. Its core characteristic is parallel computing. Some works adopt the type of attention mechanism to video summarization. Fajtl et al. [25] use self-attention mechanism to perform the entire sequence-to-sequence transformation in video summarization task. Ji et al. [53] incorporate a self-attention mechanism in the encoder to capture the short-term contextual information. Li et al. [22] propose a global diverse attention mechanism by adapting self-attention mechanism to estimate diverse attention weights, and then transform them to importance scores. But unlike the three works in which computationally demanding LSTM or CNN, as well as full attention, is exploited, our work has no LSTM and CNN operations, and uses local-global sparse attention instead of full attention to train model.

More recently, some works strictly following standard self-attention have been proposed. Its core property is the scaled dot-product attention and multi-head attention mechanism. The former is used to model dependencies between all tokens of a sequence, while the latter allows the model to attend to different representation subspaces. Li et al. [11] use the type

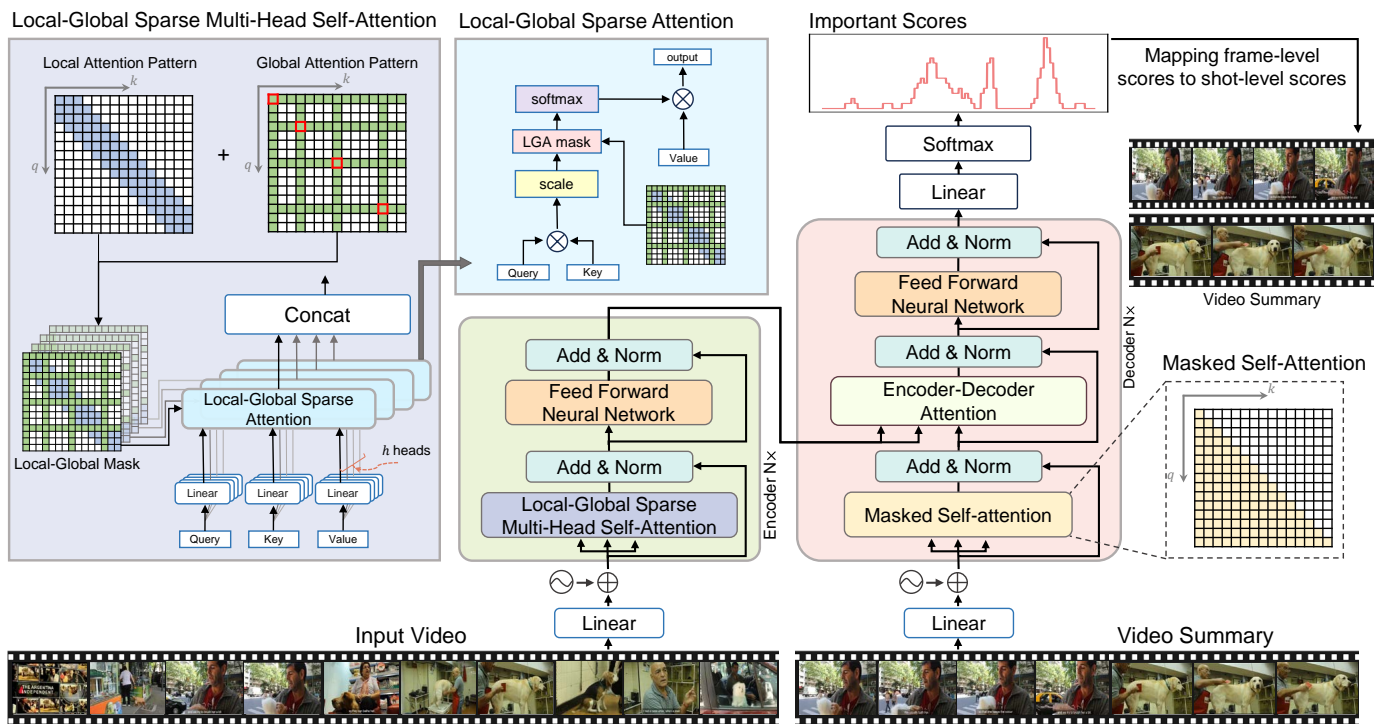


Fig. 2. The whole overview of FullTransNet architecture. It follows vanilla transformer with full encoder-decoder structure and exploits local-global sparse attention instead of standard full attention to build the network. The local-global sparse attention is a combination of local attention and global attention, and only used at the encoder side. Based on this sparse attention mechanism, local-global sparse multi-head attention is designed to yield a better output representation.

of attention mechanism to explicitly model cross-video high-level patterns for video co-summarization. Hsu et al. [23] use temporal and spatial attention to achieve a good summarization performance. This mechanism is standard self-attention and just performed at the encoder side, since its model is encoder-only architecture, while our attention includes sparse attention at the encoder, masked self-attention and cross attention at the decoder, which is applied to full transformer architecture. Although full attention has the capability of capturing global dependencies, it results in missing inductive bias of locality. In our work, we adopt local-global sparse attention as structural prior to train the model on relatively small-scale video data. With respect to more works about attention mechanisms in computer vision, readers can refer to the related review literatures [47], [55], [56], [57], [58].

III. METHOD

Similar to [24], [25], [53], we formulate video summarization as a seq2seq learning problem. We solve this problem via a standard transformer with full encoder-decoder structure. In addition, taking into account the model efficiency, we use local-global sparse attention instead of full attention to balance the performance and efficiency. Our proposed model architecture, namely FullTransNet, takes the two techniques as main building blocks, as shown in Fig. 2. In this section, we will elaborate on each building technique used by our model, including the encoder-decoder structure, sparse attention mechanism, as well as other components of our whole method such as the training process.

A. Model Architecture

1) *Encoder with Local-Global Sparse Attention*: In neural machine translation tasks, it is natural to encode input word sequences, transforming the vocabulary and structure of the input sentence into a continuous semantic representation. We apply this idea to the video summarization task, in which each video frame is considered as a word in a sentence. Thus, similar to the word sequence, the frame sequence in a video is encoded to a continuous latent representation.

We use the vanilla transformer [28] as our base architecture, in which the encoder is a crucial component. The encoder consists of N stacked layers. Each encoder layer, except for the first one, takes as its input the output of the previous encoder layer. Each encoder layer performs a series of transformations on input sequences, progressively extracting higher-level semantic information suitable for summarization. When encoding a frame sequence, the transformer not only maps the sequence to a latent space but also can capture the dependencies between frames through the attention mechanism.

In addition, we apply linear projection to obtain embedded features from the features of each video frame extracted by GoogLeNet [44] to keep in step with the embedding operation in the translation task and to reduce the dimensionality of video features from 1024 to d . Then, we incorporate positional encoding the same as one in the vanilla transformer to enable the network to perceive the spatial position information.

In brief, the encoder can be formulated as:

$$\text{encoder}(\mathbf{Z}_{enc}) = \begin{cases} f_{enc}^i(\mathbf{Z}_{enc} + \mathbf{P}_{enc}), & i = 1 \\ f_{enc}^i(\mathbf{Y}_{enc}^{i-1}), & 2 \leq i \leq N \end{cases}, \quad (1)$$

where $\mathbf{P}_{enc} \in \mathbb{R}^{T \times d}$ represents the positional encoding, which has the same shape as the embedded representation \mathbf{Z}_{enc} , and f_{enc}^i denotes the i -th encoder layer. \mathbf{Y}_{enc}^{i-1} represents the output of the $(i-1)$ -th encoder layer. T and d are the number of frames in the original video and the representation dimensionality, respectively. The structure of the first encoder layer is shown in Fig. 2 (bottom). Concretely, each encoder layer has two sub-layers: a multi-head self-attention with local-global sparse attention and a position-wise fully connected feed-forward network (FFN), in which the multi-head self-attention with local-global sparse attention is called as **Local-Global Sparse Multi-Head Self-Attention** mechanism (LGS-MHSA) in this paper. In addition, following the vanilla transformer [28], a residual connection [46] is used around each sub-layer, followed by layer normalization [59]. Thus, the output of the two sub-layers (denoted as $\mathbf{X}'_i \in \mathbb{R}^{T \times d}$ and $\mathbf{X}''_i \in \mathbb{R}^{T \times d}$) in the i -th encoder can be expressed as follows:

$$\mathbf{X}'_i = \text{LayerNorm}(\text{LGS-MHSA}(\mathbf{X}_i, \mathbf{X}_i, \mathbf{X}_i) + \mathbf{X}_i), \quad (2)$$

$$\mathbf{X}''_i = \text{LayerNorm}(\text{FFN}(\mathbf{X}'_i) + \mathbf{X}'_i), \quad (3)$$

where $\mathbf{X}_i \in \mathbb{R}^{T \times d}$ indicates the output of the $(i-1)$ -th encoder, i.e., \mathbf{Y}_{enc}^{i-1} .

LGS-MHSA(\cdot) means multi-head self-attention with local-global sparse mechanism, which is an updated version of vanilla multi-head self-attention (MHSA) [28], where the local-global sparse mechanism is used to add a locality prior to the original input sequence and to set some positions as global tokens to attend to all tokens in the sequence. With respect to the reasons for doing this, we will give a detailed specification and explanation in subsection III-B.

Except for the LGS-MHSA sub-layer, an identical position-wise fully connected feed-forward network (FFN) is applied to each position. The FFN has two linear transformations with a ReLU activation in between, which is the same as the vanilla transformer [28].

$$\text{FFN}(\mathbf{X}'_i) = \max(0, \mathbf{X}'_i \mathbf{W}_1 + b_1) \mathbf{W}_2 + b_2. \quad (4)$$

2) *Decoder*: The decoder is also built upon the self-attention mechanism, but it does not employ the proposed local-global sparse attention. The whole decoder block consists of N decoder layers, of which the number is identical to that of encoder layers. The input to the first decoder layer is the summary sequence along with positional encoding. Except for the first decoder layer, each layer's input includes two parts: the output from the previous decoder layer and the contextual representations from the encoder. The contextual representations contain inter-frame relationship information from the original input sequence, which is exploited by the decoder to effectively generate the target sequence. The decoder can be expressed as:

$$\text{decoder}(\mathbf{Z}_{dec}, \mathbf{Y}_{enc}^N) = \begin{cases} f_{dec}^i(\mathbf{Z}_{dec} + \mathbf{P}_{dec}, \mathbf{Y}_{enc}^N), & i = 1 \\ f_{dec}^i(\mathbf{Y}_{dec}^{i-1}, \mathbf{Y}_{enc}^N), & 2 \leq i \leq N \end{cases}, \quad (5)$$

where $\mathbf{P}_{dec} \in \mathbb{R}^{L \times d}$ represents the positional encoding, which has the same shape as the embedded representation \mathbf{Z}_{dec} . \mathbf{Y}_{enc}^N means the output of the last encoder layer, and f_{dec}^i

denotes the i -th decoder layer. \mathbf{Y}_{dec}^{i-1} represents the output of the $(i-1)$ -th decoder layer. L and d are the lengths of the summary sequence formed by keyframes and the representation dimensionality, respectively. The structure of the first decoder is shown in Fig. 2 (bottom). Concretely, Each decoder layer primarily consists of three sub-modules: masked multi-head self-attention (MMHSA), i.e., causal attention, encoder-decoder attention, i.e., cross attention (CA), and a position-wise fully connected feed-forward network (FFN). Similar to the encoder, a residual connection [46] is used around each sub-layer, followed by layer normalization [59]. Thus, the output of the three sub-layers (denoted as $\mathbf{S}'_i \in \mathbb{R}^{L \times d}$, $\mathbf{S}''_i \in \mathbb{R}^{L \times d}$, and $\mathbf{S}'''_i \in \mathbb{R}^{L \times d}$) in the i -th decoder can be expressed as follows:

$$\mathbf{S}'_i = \text{LayerNorm}(\text{MMHSA}(\mathbf{S}_i, \mathbf{S}_i, \mathbf{S}_i) + \mathbf{S}_i), \quad (6)$$

$$\mathbf{S}''_i = \text{LayerNorm}(\text{CA}(\mathbf{Y}_{enc}^N, \mathbf{Y}_{enc}^N, \mathbf{S}'_i) + \mathbf{S}'_i), \quad (7)$$

$$\mathbf{S}'''_i = \text{LayerNorm}(\text{FFN}(\mathbf{S}''_i) + \mathbf{S}''_i), \quad (8)$$

where $\mathbf{S}_i \in \mathbb{R}^{L \times d}$ shows the output of the $(i-1)$ -th decoder, i.e., \mathbf{Y}_{dec}^{i-1} . CA(\cdot) receives the inputs from both the encoder and the decoder. MMHSA(\cdot) allows each query \mathbf{Q} to only attend to all the keys \mathbf{K} and values \mathbf{V} at the current query position and its preceding positions. This is typically implemented through a masked function applied on the unnormalized attention matrix $\hat{\mathbf{A}} = \exp(\frac{\mathbf{Q}\mathbf{K}^T}{\sqrt{d}})$, which can enable parallel computation in training. All the values at the positions that do not need to be attended to are set to $-\infty$, i.e., $\hat{\mathbf{A}}_{mn} = -\infty$ if $m < n$. This masked self-attention ensures that the information after the current position is not fed to the decoder, which thus remains the auto-regressive property of the video summarization task.

Additionally, the encoder-decoder attention module allows the decoder to access the entire output of the encoder. Using the context of the input sequence can help to generate the next most likely keyframe. The output of the last decoder layer is passed to a linear transformation to project its dimensionality d to the length T of the original video. Subsequently, softmax function is applied to these projected values to convert them into a probability distribution, facilitating the determination of which frames are most likely selected as keyframes.

B. Local-Global Sparse Multi-Head Self-Attention

Using local-global sparse attention (LGA) instead of full attention (FA) has the two most straight purposes. First, it is used to reduce the memory footprints and computation requirements and handle longer sequences. Second, it is expected to effectively select the representative frames. Because the computation grows quadratically with sequence length in FA, which causes severe scalability issues, we propose using LGA to address this limitation. According to this fact most data, particularly video data, has a property of locality, and thus, directly using softmax mapping on all tokens, i.e., assigning a weight to all tokens, seems to be paradoxical, which is because not all tokens are relevant or are worth being attended to. Thus, it is natural to restrict each query to only attend to its neighbors. Based on this, we utilize local attention to only normalize the neighbor tokens in window w from the attention

matrix in a row-wise manner, so as to assign a larger weight to the tokens, which is very beneficial for selecting keyframes.

Other advantages of this LGA mechanism are also beneficial for our task. For example, LGA can introduce locality prior to mitigate the overfitting on small-scale datasets. Local operation maintains translation invariant, which makes this attention focus on similar or the same information across different positions. In addition, when multiple local window attention layers are stacked, the top layer can access all input information across the entire sequence, leading to a nearly full receptive field similar to vanilla self-attention, which makes it most likely to match vanilla self-attention in performance. Meanwhile, global attention in LGA is intentionally designed for learning the global representations across all frames in a sequence, which can alleviate the degradation of the ability to model the long-range dependencies using local attention. All these potential advantages motivate us to propose this LGA mechanism in our model architecture. The LGA is a combination of local attention and global attention. The local attention, global attention, and their combination patterns are shown in Fig. 1 and Fig. 2. The detailed specifications of our LGA will be given as follows.

The attention relationships of query-key pairs, as well as the connectivity matrix between all query-key pairs, are illustrated in Fig. 1 and Fig. 2. Local attention allows the model to focus on the neighbors of each frame, which helps rapidly identify keyframes. The attention computation for each query only involves elements within a small window around it, rather than the entire sequence. This means that the key-value pairs outside the window can be effectively masked out, achieving local focus and greatly reducing computation costs.

To tackle the limitations of local attention in modeling long-range dependencies, we add global attention to several key positions. In our configuration of LGA, the first, the middle, and the last positions are selected as key positions. The elements at key positions are treated as global tokens, which can attend to all elements in the sequence and vice versa, as illustrated in Fig. 1 and Fig. 2. Global attention allows the model to learn the representations of the whole sequence, which is helpful for the decoder to predict keyframes.

Based on the above analyses, the combined sparse attention can be understood as introducing an inductive bias to the input, which is helpful to effectively train the model and save computation costs. Assuming a window size of w , we formulate the local-global sparse attention as the following pre-defined patterns, and then the similarity scores of query-pairs can be computed as follows:

$$\hat{\mathbf{A}}_{mn} = \begin{cases} \frac{\mathbf{q}_m \mathbf{k}_n^\top}{\sqrt{d}}, & \text{if token } m \text{ attends to token } n \\ -\infty, & \text{else} \end{cases}, \quad (9)$$

where $\hat{\mathbf{A}}_{mn}$ is unnormalized attention matrix, m, n are indices of corresponding tokens, and $n \in [\max(0, m - \lfloor \frac{w}{2} \rfloor), \min(n - 1, m + \lfloor \frac{w}{2} \rfloor)] \cup \{f_s^{start}, f_s^{mid}, f_s^{end}\}_{s=1}^{SN}$, s is index of different shots, SN is the shot number of video, f_s^{start} , f_s^{mid} , and f_s^{end} represent the first, the middle, and the last frame of each shot. The output representation of LGA can be then computed as

follows:

$$\text{LGA}(\hat{\mathbf{A}}, \mathbf{V}) = \text{softmax}(\hat{\mathbf{A}})\mathbf{V}. \quad (10)$$

Following [28], instead of performing a single attention function LGA, Our model adopts a local-global sparse multi-head self-attention (LGS-MHSA), which allows the model to jointly attend to information from different representation subspaces at different positions. The LGS-MHSA projects d -dimensional queries \mathbf{Q} , keys \mathbf{K} , and values \mathbf{V} to d_k , d_k , and d_v dimensions by using h different sets of learned projections, respectively. The LGA attention function Eq. (10) is performed on each of the projected queries \mathbf{Q}_{d_k} , keys \mathbf{K}_{d_k} , and values \mathbf{V}_{d_v} to yield d_v -dimensional output values. The model then concatenates all the outputs and projects them back to a d -dimensional representation, as illustrated in the following equations:

$$\text{LGS-MHSA}(\mathbf{Q}, \mathbf{K}, \mathbf{V}) = \text{Concat}(\mathbf{H}_1, \dots, \mathbf{H}_h)W^O, \quad (11)$$

$$\text{where } \mathbf{H}_i = \text{LGA}(\mathbf{Q}_{d_k}, \mathbf{K}_{d_k}, \mathbf{V}_{d_v}), \quad (12)$$

where h is the number of heads in model, $\mathbf{Q}, \mathbf{K}, \mathbf{V} \in \mathbb{R}^{T \times d}$, $\mathbf{Q}_{d_k}, \mathbf{K}_{d_k}, \mathbf{V}_{d_v} \in \mathbb{R}^{T \times d_k}$, $W^O \in \mathbb{R}^{hd_v \times d}$. In this work, we use $h = 8$, and thus $d_k = d_k = d_v = d/h = 8$.

Furthermore, it is noteworthy that the sparse attention is only implemented at the encoder side, which is due to the fact that the length of the summary sequence is typically very small compared to the original input. The computational complexity of the local attention pattern is $O(n \times w)$, which scales linearly with the length n of the input frame sequence. Although global attention is adopted in this work, since the number of such tokens is relatively small and independent from n , the computational complexity of LGA is still $O(n)$.

C. Training

During training, we mainly focus on the teacher forcing method used by the decoder, which is because the decoder uses it to process the summary sequence. At each time step, instead of directly using its previous prediction, the decoder considers taking the target output sequence, i.e., ground truth, from the dataset as its input. This approach allows the model to effectively and accurately update its parameters to be learned based on the correct error backpropagation, which is beneficial to train a good model in a fast convergence way, so as to make the trained model generate the desirable summary sequence. Teacher forcing helps the model learn how to generate the next token, while the masking mechanism ensures that the model does not “cheat” by peeking at future tokens during training. The combination of the two techniques enables the model to more effectively learn how to generate accurate target sequences. Additionally, implementing the LGA sparse mechanism is non-trivial, since the local attention requires a form of banded matrix multiplication. For this, we adopt a customized CUDA kernel used by [36] to implement it.

We employ the simple and computationally efficient binary cross-entropy (BCE) loss to train model. We treated the label of each video frame as a binary classification problem to

indicate whether a frame is selected as a keyframe or not. The loss function is formally denoted as follows:

$$\mathcal{L}_{BCE}(y_n, p_n) = -\frac{1}{T} \sum_{n=1}^{L \times T} [y_n \log(p_n) + (1 - y_n) \log(1 - p_n)], \quad (13)$$

where T represents the number of video frames, and y_n denotes the ground-truth label of the n -th frame, obtained by converting importance scores into binary labels (0 and 1) at the shot level. The importance score can be interpreted as the probability p_n of a keyframe being selected. The training procedure of our FullTransNet is summarized in Algorithm 1.

Algorithm 1: The train procedure of FullTransNet

Input: Original videos \mathbf{X}_n , Frame-level importance scores \mathbf{y}_n .

Output: Video summaries \mathbf{p}_n and all the parameters θ in FullTransNet.

Initialize θ of FullTransNet using Xavier.

for $split \leftarrow 1$ **to** 5 **do**

for $epoch \leftarrow 1$ **to** E **do**

 % E indicates epoch, $E = 300$ in our work.

for $\mathbf{X} \in \{\mathbf{X}_n\}$, $\mathbf{y} \in \{\mathbf{y}_n\}$ **do**

 % key-frames summary ;

$\mathbf{s} \leftarrow \text{Knapsack [2]} (\text{KTS [60]}(\mathbf{X}), \mathbf{y})$;

$\mathbf{S} \leftarrow \mathbf{X}[\text{if } \mathbf{s} \text{ is True}]$;

$\mathbf{E}_X \leftarrow \text{embedding}(\mathbf{X}) + \mathbf{P}_{enc}(\mathbf{X})$;

$\mathbf{E}_S \leftarrow \text{embedding}(\mathbf{S}) + \mathbf{P}_{dec}(\mathbf{S})$;

$\mathbf{Y}_{enc}^{N-1} \leftarrow \text{encoder}(\mathbf{E}_X)$;

$\mathbf{Y}_{enc}^N \leftarrow \text{encoder}(\mathbf{Y}_{enc}^{N-1})$;

$\mathbf{Y}_{dec}^{N-1} \leftarrow \text{decoder}(\mathbf{E}_S, \mathbf{Y}_{enc}^N)$;

$\mathbf{Y}_{dec}^N \leftarrow \text{decoder}(\mathbf{E}_S, \mathbf{Y}_{dec}^{N-1})$;

$\mathbf{p} \leftarrow \text{softmax}(\text{Linear}(\mathbf{Y}_{dec}^N))$;

$\mathbf{p}_n \leftarrow \text{ScoretoKeyFrame}(\mathbf{p})$;

$\mathcal{L} \leftarrow \mathcal{L}_{BCE}(\mathbf{y}_n, \mathbf{p}_n)$;

 % i.e., loss in Eq. (13) ;

$\theta \leftarrow \theta - \alpha \frac{\partial \mathcal{L}}{\partial \theta}$;

end

end

end

IV. EXPERIMENTS AND RESULTS

A. Datasets

Two public benchmark datasets: SumMe [1] and TVSum [2] for video summarization are used to evaluate the proposed method. SumMe consists of 25 user videos ranging from 1 to 6 minutes in length and provides multiple user-annotated summaries (by 15-18 different users) for each video in the form of key shots. The dataset covers multiple events from both first-person and third-person cameras, such as holidays, cooking, and sports. TVSum contains 50 videos with 10 categories (5 videos per category), which vary from 2 to 10 minutes in length and are annotated by 20 users in the form of frame-level importance scores. Similar to SumMe, the dataset also covers

various genres such as beekeeping, making sandwiches, and grooming an animal. Since our method is based on supervised learning, more annotated data is more beneficial to the training. Thus, two other annotated datasets with keyframes: OVP [14] and YouTube [14] are used as augmented training datasets. OVP has 50 videos with various genres varying from 1 to 10 minutes in length, while YouTube consists of 39 videos with multiple visual styles excluding cartoons, whose lengths are from 1 to 4 minutes. The descriptions of four datasets are shown in Table I.

Following previous works [4], [11], [24], [19], [52], we apply three commonly used settings, i.e., canonical, augmented, and transfer, to train and evaluate our model. Concretely, in the canonical setting, with respect to SumMe and TVSum, training and testing sets are from the same dataset between them. Each dataset is randomly divided into 5 disjoint splits, and 80% of each dataset is used for training, and the remaining 20% is used for evaluation. In the augmented setting, YouTube and OVP are added to the training set, and the testing set remains the same. As for the transfer setting, YouTube, OVP, and TVSum (SumMe) are used as the training set, and SumMe (TVSum) is used as the testing set.

Since our model requires ground truth key shots, thus for TVSum dataset that only provides frame-level importance scores, following [4], we convert the frame-level importance scores into key shots.

B. Evaluation Metrics

For a fair comparison with other previous works [4], [11], [24], [25], we adopt F-Measure (a.k.a. F-score) as the valuation metric. Given a video V , V_{gt} and V_{gs} represent its ground-truth summary and generated summary, respectively. Precision(P) and recall (R) are then calculated based on the length of temporal overlap between V_{gt} and V_{gs} as follows:

$$P = \frac{|V_{gt} \cap V_{gs}|}{|V_{gs}|}, R = \frac{|V_{gt} \cap V_{gs}|}{|V_{gt}|}, \quad (14)$$

where $V_{gt} \cap V_{gs}$ denotes temporal overlap between them, and $|\cdot|$ indicates the length of temporal duration. The harmonic mean F-Measure is then computed with P and R as follows:

$$F = \frac{2PR}{P+R} \times 100\%. \quad (15)$$

A higher F-Measure means more temporal overlaps between the generated summary and ground-truth summary while keeping less redundancy.

C. Experimental settings

We train our FullTransNet and its various ablation variants on an NVIDIA 3090 graphics card with 24GB memory. We implement our approach using Python 3.10 and PyTorch 2.0 [61]. We train all models using Adam [62] optimizer for 300 epochs from scratch on corresponding datasets in three different settings, with a batch size of 1, learning rate of $1e-3$, momentum of 0.9, and weight decay of $1e-4$. Training one model takes 5–8 hours. We set the size of the sliding window to 17, that is, each token attends to 8 tokens on both sides

TABLE I
THE DESCRIPTIONS OF DATASETS USED IN THE EXPERIMENTS. “# FRAMES” INDICATES THE NUMBER OF FRAMES IN ALL SHOTS.

Dataset	# Videos	Duration (min)	Genres/Topics	Annotations	# Frames (Min,Max,Avg)
SumMe [1]	25	1–6	Holidays and Sports	Key shots	7, 2133, 146
TVSum [2]	50	2–10	News Coverage, and Bee Activities	Frame-level important scores	10, 997, 148
OVP [14]	50	1–10	Cartoons, Commercials, and Home Videos	Keyframes	29, 1289, 213
YouTube [14]	39	1–4	Documentary, Educational, and Lecture	Keyframes	15, 3780, 221

of itself. Empirically, the tokens in this attention span have proved to be most relevant. Additionally, we set the feature dimension of the token as 64. The main aim of doing this is to achieve a trade-off between computation efficiency and model complexity. In this task, since the maximum length of videos in all datasets is 1,513 frames, to accommodate all video frames and compute weight matrices, we set the sequence length to 1,536. As for these sequences whose length is less than the maximum value, we pad “0” into the corresponding positions in these sequences to keep the length of each video sequence identical.

Besides, by convention [4], [11], [24], [19], all videos are downsampled from 30 fps to 2 fps to remove redundancy. The output of the pool5 layer of GoogLeNet [44] pre-trained on ImageNet [63] is used as the feature descriptor of each video frame. Five-fold cross-validation for each setting is performed to yield an average performance.

D. Comparisons with Existing Methods

In this section, we compare the proposed FullTransNet with several existing methods on SumMe and TVSum in terms of F-Measure. Among these representative works, vsLSTM [4], dppLSTM [4], H-RNN [5], HSA-RNN [6], TTH-RNN [20], and SUM-FCN [18] primarily adopt RNN or CNN as core building techniques, while A-AVS [24], M-AVS [24], vsLSTM+Att [26], dppLSTM+Att [26], SUM-GAN-AAE [3], and DASP [52], as well as VASNet [25], SUM-GDA_{sup} [22], H-MAN [27], DMASum [54], VJMHT [11], and STVT [23] use attention mechanism as key building units, in which these methods [11], [22], [23], [25], [27], [54] utilize transformer attention, and the others utilize non-transformer attention.

The quantitative comparisons of results are shown in Table II. It can be seen that the summarization performance of models with attention consistently surpasses that of other models without attention under almost all the three commonly used settings, i.e., canonical, augmented, and transfer settings. It shows that the attention mechanism is capable of modeling long-range dependency in sequence data of video, which is of central importance for the performance-boosting of video summarization tasks. Furthermore, there is a similar observation between non-transformer and transformer attention, in which transformer attention typically outperforms non-transformer on the summarization performance. We believe that the reason may be because the self-attention mechanism [28] without recurrence and convolution operations can learn better representation in sequences relative to other attentions. More concretely, one can see that our FullTransNet outperforms almost all the existing approaches on both two datasets under

all three settings except for DASP [52] and DMASum [54]. DASP [52] slightly improves by 0.4% solely on TVSum under the augmented settings, while our method significantly surpasses DASP [52] on SumMe by 8.9% and 7.6% under both the canonical and augmented settings, respectively, even on TVSum by 0.3% under the augmented settings. This clearly shows that our methods can achieve a well-balanced performance on the two datasets, verifying its effectiveness and advancement, while DASP [52] may be a method for specific datasets. DMASum [54] outperforms our method by 1.2% and 1.3% on both SumMe and TVSum only under the transfer settings. We conjecture that FullTransNet may have overly learned these different types of video data due to its relatively high network capacity which leads to a low generalization ability.

E. Ablation Study

In this section, we conduct an extensive ablation study on both two datasets under the canonical setting, to thoroughly evaluate the impact of each component involved in FullTransNet on the performance. Specifically, we study and analyze the impact of local-global sparse attention (LGA) module, the number of encoder layers with LGA, the dimension of hidden layer in FFN, the dimension of frame embedding, and the number of heads in LGS-MHSA, window size (WS) in local attention (LA), and the number of global tokens in global attention (GA). All settings are the same as those mentioned in subsection IV-C unless specified otherwise.

1) *Impact of Local-Global Sparse Attention Module*: The main purpose of conducting this ablation is to test the impact of different sparse attention patterns, including LA, GA, and LGA, and to compare sparse attention with full attention (FA) on the summarization performance. The results are shown in Table III. It can be seen that FA generally yields better results compared to LA and GA, but it has a higher computational complexity, leading to significant computational and memory overhead. Additionally, LGA, a combination of LA and GA, achieves the best F-Measure by 54.4% and 63.9% on SumMe and TVSum datasets, respectively, and compared to FA, it has a lower computation cost, a shorter inference time, and a less memory footprint. The superior performance indicates that our LGA module has a considerable advantage in modeling long-term dependencies and saving computing and memory costs. This is beneficial for improving the performance in long sequence modeling tasks such as video summarization and text summarization. The observation and finding are also consistent with that in BigBird [35] used for text summarization. It is worth noting that the FLOPs, runtime, and memory are

TABLE II

THE F-MEASURE (%) OF DIFFERENT METHODS UNDER THREE SETTINGS. THE BEST AND THE SECOND-BEST RESULTS ARE IN **BOLD** AND UNDERLINED, RESPECTIVELY. * INDICATES THAT THE RESULTS ARE REPRODUCED USING PUBLICLY AVAILABLE CODE UNDER THE SAME GOOGLERNET FEATURE DESCRIPTOR AND DOWN-SAMPLING STRATEGY SETTINGS AS OTHER METHODS FOR A FAIR COMPARISON. † DENOTES THAT SINCE WE DO NOT FIND THE CORRESPONDING CODE, HERE THE LISTED RESULTS ARE FROM THE PUBLISHED PAPER, WHOSE METHOD USES THE VGG-16 FEATURE DESCRIPTOR BUT ADOPTS THE SAME DOWN-SAMPLING STRATEGY AS ALL OTHER METHODS.

Method	Main Techniques	SumMe			TVSum		
		Canonical	Augmented	Transfer	Canonical	Augmented	Transfer
vsLSTM [4]	RNN or CNN	37.6	41.6	40.7	54.2	57.9	56.9
dppLSTM [4]		39.6	42.9	41.8	54.7	59.6	58.7
H-RNN [5]		44.3	–	–	62.1	–	–
HSA-RNN† [6]		44.1	–	–	59.8	–	–
TTH-RNN [20]		45.0	–	–	62.3	–	–
SUM-FCN [18]		47.5	51.1	44.1	56.8	59.2	58.2
A-AVS [24]	Non-Transformer Attention	43.9	44.6	–	59.4	60.8	–
M-AVS [24]		44.4	46.1	–	61.0	59.1	–
vsLSTM+Att [26]		43.2	–	–	63.1	–	–
dppLSTM+Att [26]		43.8	–	–	53.9	–	–
SUM-GAN-AAE [3]		48.9	–	–	58.3	–	–
DASP [52]		45.5	47.0	–	<u>63.6</u>	64.5	–
VASNet [25]	Transformer Attention	49.7	51.1	–	61.4	62.3	–
SUM-GDA _{sup} [22]		52.8	<u>54.4</u>	46.9	58.9	60.1	59.0
H-MAN [27]		51.8	52.5	48.1	50.4	61.0	59.5
DMASum [54]		<u>54.3</u>	54.1	52.2	61.4	61.2	60.5
VJMHT [11]		50.6	51.7	46.4	60.9	61.9	58.9
STVT* [23]		50.8	–	–	61.7	–	–
FullTransNet (ours)		54.4	54.6	<u>51.0</u>	63.9	<u>64.1</u>	<u>59.2</u>

TABLE III

COMPARISONS ON F-MEASURE (%) OF DIFFERENT ATTENTION PATTERNS ON SUMME AND TVSUM. FA REPRESENTS FULL ATTENTION. LA AND GA DENOTE LOCAL ATTENTION AND GLOBAL ATTENTION, RESPECTIVELY. LGA MEANS A COMBINATION OF LOCAL ATTENTION AND GLOBAL ATTENTION. NOTE THAT ALL ATTENTION PATTERNS ONLY BE ADOPTED AT THE ENCODER SIDE; ALL EVALUATIONS ARE PERFORMED UNDER THE CANONICAL SETTING. OTHER PARAMETERS ARE THE SAME AS THOSE OF FULLTRANSNET IN TABLE IV.

Dataset	Attention Pattern				F-Measure	Params (M)	FLOPs (G)	Runtime (s)	Memory (GB)
	FA	LA	GA	LGA					
SumMe	✓	–	–	–	52.67	3.613	2.785	1.345	0.171
	–	✓	–	–	53.86	3.525	2.583	0.005	0.030
	–	–	✓	–	51.91	3.525	2.639	0.007	0.031
	–	–	–	✓	54.40	3.538	2.672	0.117	0.038
TVSum	✓	–	–	–	62.75	3.613	2.899	2.338	0.171
	–	✓	–	–	62.12	3.525	2.697	0.019	0.030
	–	–	✓	–	61.82	3.525	2.753	0.050	0.032
	–	–	–	✓	63.94	3.538	2.786	0.179	0.039

calculated with the 18-th video of SumMe and the 45-th video of TVSum, respectively. The former consists of 149 frames, with 44 frames executing global attention, while the latter contains 166 frames, with 51 frames executing global attention.

2) Impact of the Number of Encoder Layers with LGA:

Empirically, a greater number of encoder layers generally means the model has stronger representation ability because more layers in the encoder can capture more complex and higher-level features, and more layers in the decoder allow the model to consider more contextual information, leading to more accurate results. However, a bigger model requires more computational cost, and could potentially result in over-fitting issues. Thus, we conduct this ablation to demonstrate how different numbers of layers affect the model performance.

In this ablation, the number of layers in the encoder and decoder is set to 2, 4, 6, and 8, respectively. From Table IV rows (A), it can be observed that as the number of layers in the encoder and decoder increases, the performance gradually improves on SumMe, and the best result can be achieved by the FullTransNet with 6 layers in both encoder and decoder. But under an 8-layer setting, the performance drops significantly, which implies over-fitting. As for the number of layers, there is a similar observation on TVSum, with only an exception where the model with 2 layers slightly improves by 0.01% compared to the model with 4 layers. We believe that this reason should be attributed to the dataset itself. The distribution of data on SumMe may be more uniform, which is beneficial for model training. Therefore, the encoder with 6 layers is used throughout all the experiments.

TABLE IV

PERFORMANCE COMPARISONS ON F-MEASURE (%) OF FULLTRANSNET ARCHITECTURE AND ITS ABLATION VARIANTS ON SUMME AND TVSUM. DEFAULT VALUES ARE IDENTICAL TO THOSE OF THE FULLTRANSNET MODEL. ALL EVALUATIONS ARE PERFORMED UNDER THE CANONICAL SETTING.

	N	d	d_{ff}	h	d_k	d_v	WS in LA	# Tokens in GA	SumMe	TVSum
(A)	2								50.6	63.1
	4								52.9	63.0
	8								51.3	62.7
(B)		32			4	4			51.1	63.0
		256			32	32			49.7	59.6
		512			64	64			44.8	57.8
		1024			128	128			46.6	56.9
(C)			512						52.4	64.0
			1024						52.2	63.8
(D)				1	64	64			45.7	60.1
				4	16	8			48.9	62.8
(E)							9		49.8	63.9
							65		53.3	63.7
							129		52.2	63.3
(F)								1	52.7	62.8
								2	53.0	63.1
FullTransNet	6	64	2048	8	8	8	17	3	54.4	63.9

3) *Impact of the Dimension of Frame Embedding:* The dimension of frame embeddings is important to the performance of the model. In this section, we conduct this ablation on the dimension of token embeddings to evaluate the performance of the model with different dimension settings. The results generated using five different dimensions: 32, 64, 256, 512, and 1,024, are shown in Table IV rows (B). It can be seen that when this dimension is set as 64, the performance reaches the best on the two datasets, while after that, the performance is nearly gradually decreased as the dimension increases. We believe that over-fitting could occur in those cases. Thus, we set the dimension as 64 and use it for all the experiments.

4) *Impact of the Dimension of Hidden Layer in FFN:* In the ablation study, our main purpose is to explore how different dimensions (d_{ff}) of the middle hidden layer in the feedforward network affect the performance of the network. We vary the number of neurons in the hidden layer to measure the performance. By comparing the performance of models with different dimensions of the hidden layer, we aim to achieve the best performance under a specific value of d_{ff} . The results are shown in Table IV rows (C). One can see that the performance on the two datasets is consistently decreasing when the dimensionality d_{ff} changes from 512 to 1,024, while the performance can be consistently improved when the dimensionality d_{ff} goes from 1,024 to 2,048. We believe the reason is that when the d_{ff} is fixed to 1,024, other parameters may not be the optimal hyperparameters, thus making the model trapped in a local optimum; on the contrary, when d_{ff} is set to 2,048, combined with other parameters, which makes it possible to learn an optimal model with good generalization ability. Therefore, we set the dimension of the hidden layer in FFN to 2,048 in our FullTransNet model.

5) *Impact of the Number of Heads in LGS-MHSA:* In this section, we will explore the impact of the number of heads in the local-global sparse multi-head self-attention (LGS-MHSA) mechanism on performance. The results are shown in Table IV rows (D). As we can see the performance can be gradually improved on both datasets as the number of heads increases, and using 8 heads achieves the best results. This reason may be that more heads in LGS-MHSA attend to more information at different positions from different representation subspaces, which could enhance the representation ability of the model. The visualization of the information attended by 8 heads in each layer at different positions is detailed in subsection IV-E8. The qualitative results show how the query token focuses on the information at different positions.

6) *Impact of Window Size in Local Attention:* To show the importance of window size in local attention, we investigate the impact of window size using different configurations of 9, 17, 65, and 129, and report the experimental results in Table IV rows (E). It can be seen that using a window size of 17 achieves the best results on both SumMe and TVSum datasets; when using window sizes of 65 and 129, the performance seems to be gradually decreasing, while using a window size of 9, the best performance can be achieved only on TVSum. The observation demonstrates that modeling short-term dependencies is more crucial than modeling long-term dependencies for video summarization. The reason may be that if the window size is too large, the attention may be spread to many irrelevant tokens, distracting from the key local information. The distracting attention can prevent the model from effectively capturing the information of important tokens, resulting in decreased accuracy. This assumption can be proved by the evidence from Table II. One can see that our LA achieves results on par with or better than FA on

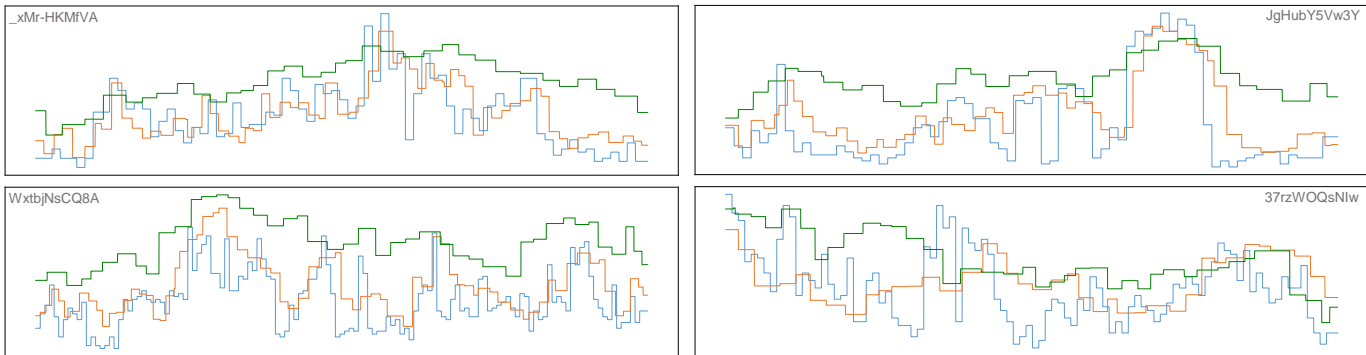


Fig. 3. Comparisons between the predicted importance scores by FullTransNet with LGA and with FA, and the ground truth importance scores on four videos from the TVSum dataset. Each subplot corresponds to one video and displays three score lines across the whole video frames, where the orange line, the green line, and the blue line represents the generated scores by FullTransNet with LGA, FullTransNet with FA, and ground-truth scores, respectively. The name of each video is placed at the top left or top right corner.

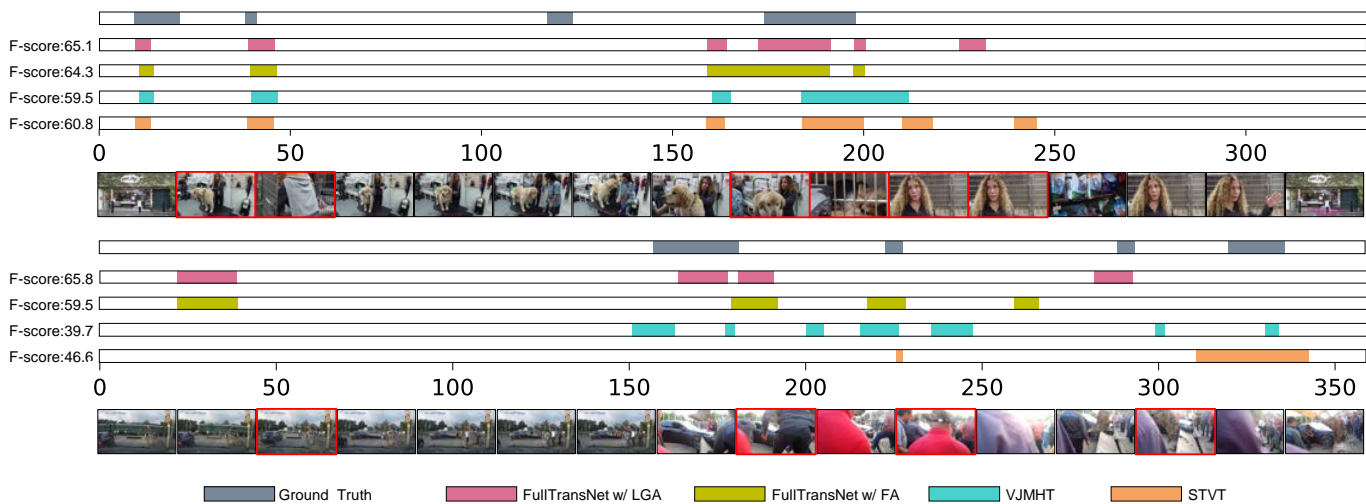


Fig. 4. Qualitative comparisons of different summarization methods, including ground truth, FullTransNet with LGA and FA, VJMHT [11], and recent STVT [23] on the 11-th video from TVSum (top) and the 6-th video from SumMe (bottom). The x-axis represents the frame indexes. Different colors in the bar are used to represent summaries generated by different methods. The frames generated by LGA as summary ones are highlighted with red boxes, sampled every 20 frames from the videos.

both datasets. This is consistent with the common sense that, for video summarization tasks, a keyframe is more relevant to the frames in its neighborhood than to all frames in the whole sequence, especially for extractive summarization tasks. Thus, for all the experiments, we use the fixed configuration of $WS = 9$.

7) *Impact of the Number of Tokens in Global Attention:* The impact of the number of tokens in global attention is shown in Table IV rows (F). We can see that as the number of tokens increases, the performance is also improved. However, this does not mean that a higher number of tokens has a better performance. The evidence from Table II can support the viewpoint. As mentioned in Method section III, we only take the first, the middle, and the last frame of a shot as the global tokens. Here the number of tokens 1, 2, and 3 refers to only using the first frame, both the first and middle frames, as well as all three frames, respectively.

8) *Attention Maps:* To better understand how attention, particularly local-global sparse attention works, we visualized the attention maps of the encoder, decoder, and encoder-

decoder, as shown in Fig. 5, Fig. 6, Fig. 7, and Fig. 8.

F. Visualization

1) *Predicted Scores of FullTransNet and Its Variants:* In this section, we will give a comprehensive qualitative evaluation to intuitively demonstrate the performance of our method and its variants on the 35-th, 44-th, 36-th, and 19-th videos from the TVSum dataset. The ground truth and predicted scores by FullTransNet are illustrated in Fig. 3. The blue lines depict the ground truth scores and the orange lines show the generated scores by FullTransNet with LGA. One can see that the predicted scores fit their corresponding ground-truth ones very well on the four videos. Moreover, we also visualize the predicted important scores by FullTransNet without LGA, i.e., with FA, indicated by the green lines. It can be seen that compared to the green lines, the orange lines are closer to the ground-truth lines. This shows that LGA is beneficial for measuring the relative importance between frames and selecting most related frames as keyframes.

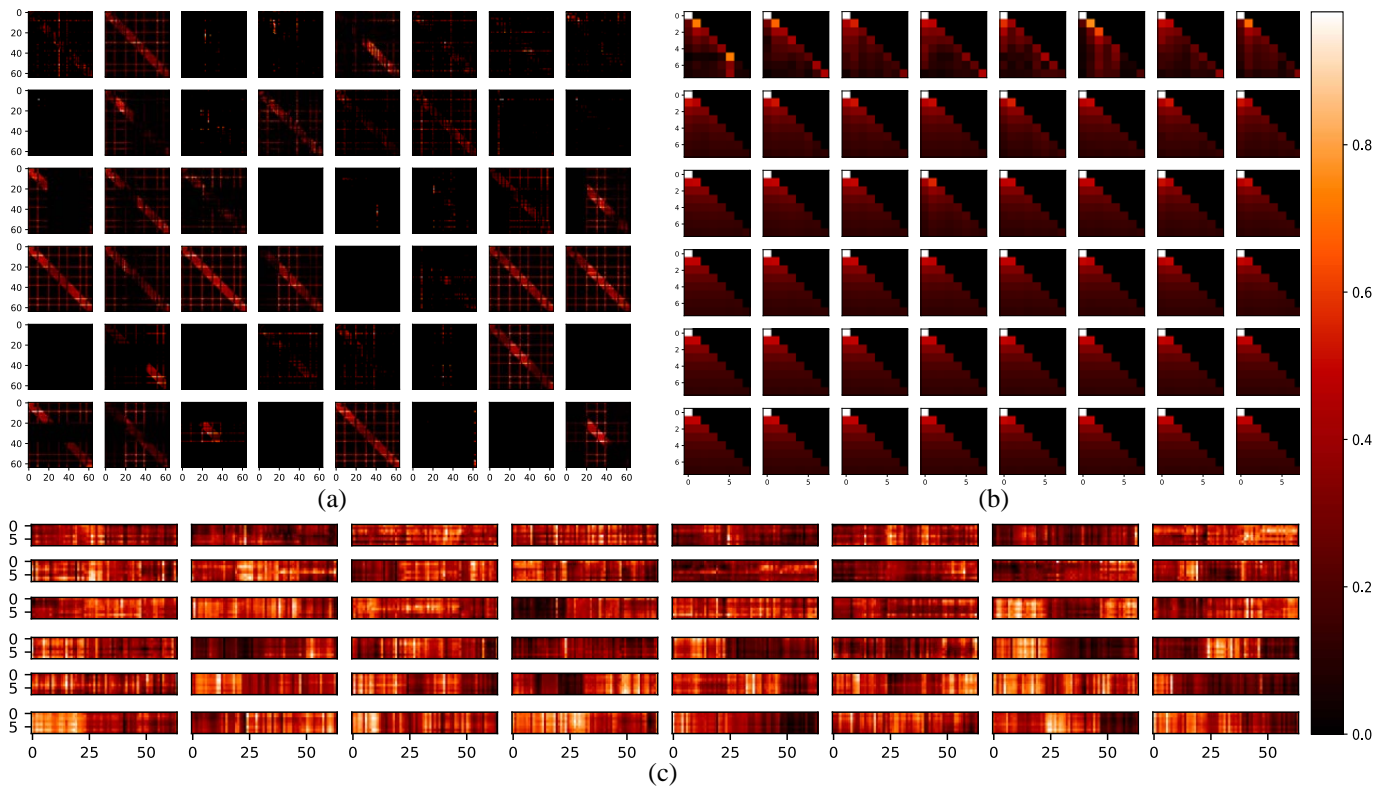


Fig. 5. Visualization of (a) LGA in encoder, (b) masked in decoder, and (c) encoder-decoder attention map for the 12-th video of SumMe, all with 6 layers and 8 heads, which is from the first epoch during training.

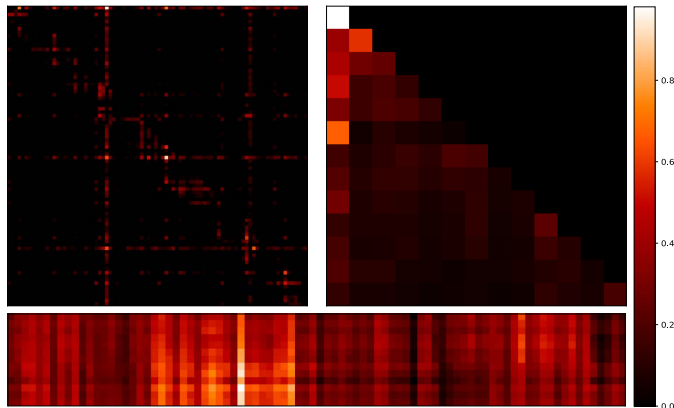


Fig. 6. Visualization of LGA (top left), masked (top right), and encoder-decoder (bottom) attention map with one head for the 8-th video of SumMe.

2) Summary Segments Generated by Different Methods:

To further understand the summarization results, we compare our proposed FullTransNet with FA and LGA with recently published VJMHT [11] and STVT [23] on the 11-th video (about animal grooming) from TVSum (top) and the 6-th video (about a car across railway) from SumMe (bottom). The qualitative results in terms of summary segments generated by different methods are shown in Fig. 4, where the results using STVT are achieved by down-sampling to 2 fps for a fair comparison. One can see that our proposed FullTransNet with FA and LGA has high overlaps with the ground truth. Although FA and LGA generate similar summary segments,

the summary segment generated by LGA seems to be close to the ground truth. Additionally, both VJMHT and STVT are nearly comparable with our FullTransNet with LGA on the 11-th video of TVSum, however, on the 6-th video of SumMe, VJMHT has fewer segments overlapping with the ground truth despite effectively distinguishing shots, on the other hand, STVT generates more concentrated summaries, which exhibits a large deviation from the ground truth. As for the reason except for the dataset itself, we believe that by using LGA instead of FA, the model no longer applies weighted averaging to all tokens, allowing it to better distinguish between different shots and select more representative key shots. Moreover, as mentioned above in Table III, LGA has lower computational complexity compared to FA. This shows the superiority of LGA on video summarization tasks.

In Fig. 5, we visualize the encoder, decoder, and encoder-decoder attention maps for the 12-th video of SumMe, where the attention weights are extracted from the model trained on SumMe dataset for one epoch under the canonical setting. Fig. 5.a, Fig. 5.b, and Fig. 5.c show the local-global sparse, masked, and cross attention maps, respectively, all with 6 layers and 8 heads. In each subfigure, rows represent layers 0–5 from top to bottom, columns represent heads 0–5 from left to right. Taking Fig. 5.a as an example, as can be seen that different heads in the same row attend to different information, for instance, for layer 4, heads 0, 2, 6–7 attend to the information of the same position, while other heads attend to the information of different position; and the information is primarily from the neighborhood of the position. The reason should be attributed

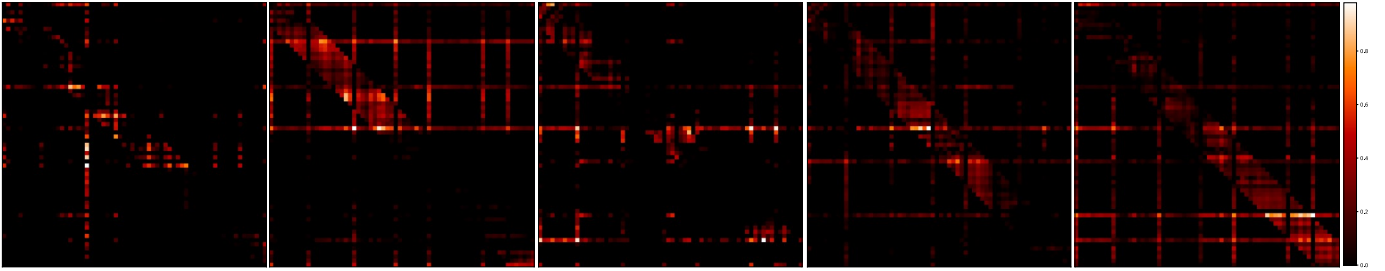


Fig. 7. Visualization of attention maps of one head for the 26-th video in TVSum at epochs 1, 50, 100, 200, and 300 from left to right, which demonstrates how the attention distribution evolves during training.

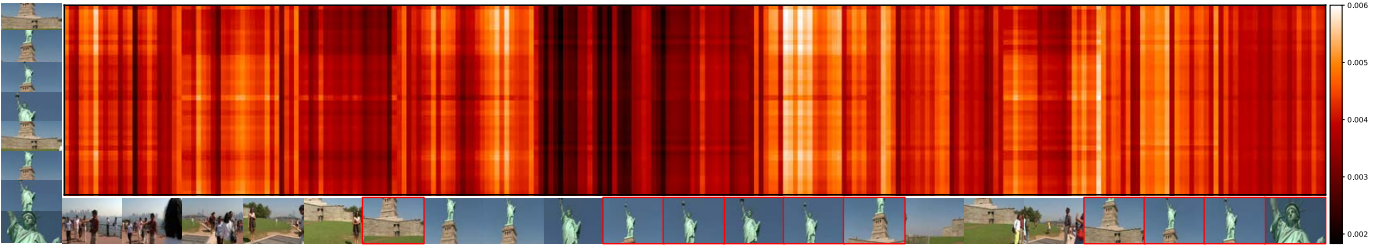


Fig. 8. Visualization of the last encoder-decoder attention map generated by FullTransNet for the 20-th video from SumMe.

to our LGS-MHSA mechanism.

To further demonstrate how one position attends to its neighbors or all corresponding tokens, we visualize the attention maps of LGA, masked, and cross-attention from layer 0 and head 0 for the 8-th video of SumMe. As can be observed from Fig. 6 a grid-like area is highlighted in the LGA attention map, which well fits with the designed attention pattern, that is, the intersecting position in this area indicates that the token at that position attends to all tokens in the sequence, while the highlighting band area shows that each token only attends to the tokens within a fixed window. The qualitative results show that applying local attention to several tokens rather than all tokens is effective. In fact, not all frames need to be attended to. The masked attention map shows that summary frames fed into the decoder present in a lower triangular style, while the cross-attention map shows that the frames being attended to present in a vertical streaks manner. This implies that there are a few indices in the output sequence that receive a greater weight for all elements in the input sequence.

Since LGA is one of our main technical contributions, to further inspect how the LGA works, we visualize the attention maps of head 0 from layer 0 at epochs 1, 50, 100, 200, and 300 for the 26-th video in TVSum, where the weights are from the models trained on TVSum under the canonical setting. One can see from Fig. 7 that the model starts to converge around 200 epochs, with the attention distribution becoming increasingly stable.

We specifically visualize the last encoder-decoder attention map for the 20-th video from SumMe to demonstrate how the attention map is affected by our LGA, as shown in Fig. 8. The horizontal axis represents the original sequence of the video, i.e., all frames of the video, while the vertical axis represents the target sequence, i.e., the sequence of keyframes. One can see that the keyframes in this exemplar are primarily located

in the middle or back part of the video; keyframes serving as the query sequence effectively focus on video frames that are similar to them (highlighted in red boxes); some target frames may concentrate on a specific frame in the original video, leading to a vertical streak through the attention-weight space, which may be because the target frames belong to one or multiple shots, where the content across these shots is relatively similar, and the particular frame happens to be within certain shot; or this frame may be mostly relevant to the target one, i.e., a frame within the keyframe sequence.

V. CONCLUSION

In this paper, we propose directly using full transformer architecture to video summarization task and introduce local-global sparse attention mechanism instead of full attention to the transformer-like network, namely FullTransNet, to achieve a comparable or even better performance against standard transformer while significantly reducing computational cost. Specifically, Similar to standard transformer, our FullTransNet also has an encoder-decoder structure, in which the encoder is responsible for transforming the original input video to key-value representations, while the decoder is tasked with addressing summary sequence with causal attention and generating an output in an auto-regressive manner. Our key contribution, the local-global sparse attention mechanism, is used only at the encoder side. Experimental results show the superiority of this structure with local-global sparse attention on video summarization against recently proposed encoder-only transformers. For future work, we will focus on how to design more sophisticated sparse mechanisms and general architecture for video summarization tasks.

REFERENCES

- [1] M. Gygli, H. Grabner, H. Riemenschneider, and L. Van Gool, "Creating summaries from user videos," in *Proc. Eur. Conf. Comput. Vis.*, Zurich, Switzerland, 2014, pp. 505–520.
- [2] Y. Song, J. Vallmitjana, A. Stent, and A. Jaimes, "TVSum: Summarizing web videos using titles," in *Proc. IEEE Conf. Comput. Vis. Pattern Recognit.*, 2015, pp. 5179–5187.
- [3] E. Apostolidis, E. Adamantidou, A. I. Metsai, V. Mezaris, and I. Patras, "Unsupervised video summarization via attention-driven adversarial learning," in *Proc. Int. Conf. MultiMedia Modeling*, vol. 26, 2020, pp. 492–504.
- [4] K. Zhang, W.-L. Chao, F. Sha, and K. Grauman, "Video summarization with long short-term memory," in *Proc. Eur. Conf. Comput. Vis.*, vol. 14, 2016, pp. 766–782.
- [5] B. Zhao, W. Liu, and X. Lu, "Hierarchical recurrent neural network for video summarization," in *Proceedings 25th ACM Int. Conf. Multimedia*, 2017, pp. 863–871.
- [6] B. Zhao, X. Li, and X. Lu, "HSA-RNN: Hierarchical structure-adaptive rnn for video summarization," in *Proc. IEEE Conf. Comput. Vis. Pattern Recognit.*, 2018, pp. 7405–7414.
- [7] X. Li, B. Zhao, and X. Lu, "A general framework for edited video and raw video summarization," *IEEE Trans. Image Process.*, vol. 26, no. 8, pp. 3652–3664, 2017.
- [8] B. Zhao, H. Li, X. Lu, and X. Li, "Reconstructive sequence-graph network for video summarization," *IEEE Trans. Pattern Anal. Mach. Intell.*, vol. 44, no. 5, pp. 2793–2801, 2022.
- [9] B. Zhao, X. Li, and X. Lu, "Property-Constrained dual learning for video summarization," *IEEE Trans. Neural Netw. Learn. Syst.*, vol. 31, no. 10, pp. 3989–4000, 2020.
- [10] D. Gupta and A. Sharma, "A comprehensive study of automatic video summarization techniques," *Artif. Intell. Rev.*, vol. 56, pp. 1–161, 2023.
- [11] H. Li, Q. Ke, M. Gong, and R. Zhang, "Video joint modelling based on hierarchical transformer for co-summarization," *IEEE Trans. Pattern Anal. Mach. Intell.*, vol. 45, no. 3, pp. 3904–3917, 2023.
- [12] Y. Zhu *et al.*, "Topic-aware video summarization using multimodal transformer," *Pattern Recognit.*, vol. 140, p. 109578, 2023.
- [13] B. Zhao, M. Gong, and X. Li, "Hierarchical multimodal transformer to summarize videos," *Neurocomputing*, vol. 468, pp. 360–369, 2022.
- [14] S. E. F. de Avila *et al.*, "VSUMM: A mechanism designed to produce static video summaries and a novel evaluation method," *Pattern Recognit. Lett.*, vol. 32, no. 1, pp. 56–68, 2011.
- [15] M. Basavarajaiah and P. Sharma, "GVSUM: generic video summarization using deep visual features," *Multim. Tools Appl.*, vol. 80, no. 9, pp. 14459–14476, 2021.
- [16] Y. Cong, J. Yuan, and J. Luo, "Towards scalable summarization of consumer videos via sparse dictionary selection," *IEEE Trans. Multimedia*, vol. 14, no. 1, pp. 66–75, 2012.
- [17] Y.-F. Ma, X.-S. Hua, L. Lu, and H.-J. Zhang, "A generic framework of user attention model and its application in video summarization," *IEEE Trans. Multimedia*, vol. 7, no. 5, pp. 907–919, 2005.
- [18] M. Rochan, L. Ye, and Y. Wang, "Video summarization using fully convolutional sequence networks," in *Proc. Eur. Conf. Comput. Vis.*, 2018, pp. 358–374.
- [19] B. Mahasseni, M. Lam, and S. Todorovic, "Unsupervised video summarization with adversarial LSTM networks," in *Proc. IEEE Conf. Comput. Vis. Pattern Recognit.*, 2017, pp. 2982–2991.
- [20] B. Bin, Zhao, X. Li, and X. Lu, "TTH-RNN: Tensor-train hierarchical recurrent nneural nnetwork for video ssummarization," *IEEE Trans. Ind. Electron.*, vol. 68, no. 4, pp. 3629–3637, 2020.
- [21] W. Zhu, Y. Han, J. Lu, and J. Zhou, "Relational reasoning over spatial-temporal graphs for video summarization," *IEEE Trans. Image Process.*, vol. 31, pp. 3017–3031, 2022.
- [22] P. Li, Q. Ye, L. Zhang, L. Yuan, X. Xu, and L. Shao, "Exploring global diverse attention via pairwise temporal relation for video summarization," *Pattern Recognit.*, vol. 111, p. 107677, 2021.
- [23] T.-C. Hsu, Y.-S. Liao, and C.-R. Huang, "Video summarization with spatiotemporal vision transformer," *IEEE Trans. Image Process.*, pp. 3013–3026, 2023.
- [24] Z. Ji, K. Xiong, Y. Pang, and X. Li, "Video summarization with attention-based encoder-decoder networks," *IEEE Trans. Circuits Syst. Video Technol.*, vol. 30, no. 6, pp. 1709–1717, 2019.
- [25] J. Fajtl, H. S. Sokeh, V. Argyriou, D. Monekosso, and P. Remagnino, "Summarizing videos with attention," in *Proc. Asian Conf. Comput. Vis.*, 2019, pp. 39–54.
- [26] L. L. Casas and E. Koblenz, "Video summarization with LSTM and deep attention models," in *Proc. Int. Conf. MultiMedia Modeling*, 2019, pp. 67–79.
- [27] Y.-T. Liu, Y.-J. Li, F.-E. Yang, S.-F. Chen, and Y.-C. F. Wang, "Learning hierarchical self-attention for video summarization," in *Proc. IEEE Int. Conf. Image Process.*, 2019, pp. 3377–3381.
- [28] A. Vaswani, N. Shazeer, N. Parmar, J. Uszkoreit, L. Jones, A. N. Gomez, L. Kaiser, and I. Polosukhin, "Attention is all you need," in *Proc. Adv. Neural Inf. Process. Syst.*, 2017, pp. 6000–6010.
- [29] T. B. Brown *et al.*, "Language models are few-shot learners," 2020. [Online]. Available: <https://arxiv.org/abs/2005.14165>
- [30] J. Devlin, M.-W. Chang, K. Lee, and K. Toutanova, "BERT: Pre-training of deep bidirectional transformers for language understanding," 2019. [Online]. Available: <https://arxiv.org/abs/1810.04805>
- [31] C. Qu, L. Lu, A. Wang, W. Yang, and Y. Chen, "Novel multi-domain attention for abstractive summarisation," *CAAI Transactions on Intelligence Technology*, vol. 8, no. 3, pp. 796–806, 2022.
- [32] U. Khandelwal, K. Clark, D. Jurafsky, and L. Kaiser, "Sample efficient subset summarization using a single pre-trained transformer," 2019. [Online]. Available: <https://arxiv.org/abs/1905.08836>
- [33] Y. Liu and M. Lapata, "Text summarization with pretrained encoders," in *Proc. Conf. Empir. Methods Nat. Lang. Process. Int. Jt. Conf. Nat. Lang. Process.*, 2019, pp. 3730–3740.
- [34] R. Child *et al.*, "Generating long sequences with sparse transformers," 2019. [Online]. Available: <https://arxiv.org/abs/1904.10509>
- [35] M. Zaheer *et al.*, "Big bird: transformers for longer sequences," in *Proc. 34th Int. Conf. Neural Inf. Process. Syst.*, 2020.
- [36] I. Beltagy *et al.*, "Longformer: The long-document transformer," 2020. [Online]. Available: <https://arxiv.org/abs/2004.05150>
- [37] B. Gong, W.-L. Chao, K. Grauman, and F. Sha, "Diverse sequential subset selection for supervised video summarization," in *Proc. 27th Int. Conf. Neural Inf. Process. Syst.*, 2014, pp. 2069–2077.
- [38] K. Zhang, K. Grauman, and F. Sha, "Retrospective encoders for video summarization," in *Proc. Eur. Conf. Comput. Vis.*, 2018, pp. 391–408.
- [39] E. Elhamifar, G. Sapiro, and S. S. Sastry, "Dissimilarity-based sparse subset selection," *IEEE Trans. Pattern Anal. Mach. Intell.*, vol. 38, no. 11, pp. 2182–2197, 2016.
- [40] Y. Yuan, H. Li, and Q. Wang, "Spatiotemporal modeling for video summarization using convolutional recurrent neural network," *IEEE Access*, vol. 7, pp. 64676–64685, 2019.
- [41] M. Elfeki and A. Borji, "Video summarization via actionness ranking," in *Proc. IEEE Winter Conf. Appl. Comput. Vis.*, 2019, pp. 754–763.
- [42] S. Lal, S. Duggal, and I. Sreedevi, "Online video summarization: Predicting future to better summarize present," in *Proc. IEEE Winter Conf. Appl. Comput. Vis.*, 2019, pp. 471–480.
- [43] A. Krizhevsky, I. Sutskever, and G. E. Hinton, "Imagenet classification with deep convolutional neural networks," *Mag. Commun ACM*, vol. 60, no. 6, pp. 84–90, 2017.
- [44] C. Szegedy, W. Liu, Y. Jia, P. Sermanet, S. Reed, D. Anguelov, D. Erhan, V. Vanhoucke, and A. Rabinovich, "Going deeper with convolutions," in *Proc. IEEE Conf. Comput. Vis. Pattern Recognit.*, 2015, pp. 1–9.
- [45] K. Simonyan and A. Zisserman, "Very deep convolutional networks for large-scale image recognition," in *Proc. Int. Conf. Learn. Represent*, San Diego, CA, United states, Apr. 2014.
- [46] K. He, X. Zhang, S. Ren, and J. Sun, "Deep residual learning for image recognition," in *Proc. IEEE Conf. Comput. Vis. Pattern Recognit.*, 2016, pp. 770–778.
- [47] Y. Tay, M. Dehghani, D. Bahri, and D. Metzler, "Efficient transformers: A survey," *ACM Comput. Surv.*, vol. 55, no. 6, pp. 109.1–109.28, 2022.
- [48] D. Bahdanau, K. Cho, and Y. Bengio, "Neural machine translation by jointly learning to align and translate," in *Proc. Int. Conf. Learn. Represent.*, San Diego, CA, United states, 2015.
- [49] M.-T. Luong, H. Pham, and C. D. Manning, "Effective approaches to attention-based neural machine translation," in *Proc. Conf. Empir. Methods Nat. Lang. Process.*, Lisbon, Portugal, 2015, pp. 1412–1421.
- [50] A. See, P. J. Liu, and C. D. Manning, "Get to the point: Summarization with pointer-generator networks," in *Proc. 55th Annu. Meet. Assoc. Comput. Linguist.*, Vancouver, Canada, 2017, pp. 1073–1083.
- [51] J. Gu, Z. Lu, H. Li, and V. O. K. Li, "Incorporating copying mechanism in sequence-to-sequence learning," in *Proc. 54th Annu. Meet. Assoc. Comput. Linguist.*, vol. 3, Berlin, Germany, 2016, pp. 1631–1640.
- [52] Z. Ji *et al.*, "Deep attentive and semantic preserving video summarization," *Neurocomputing*, vol. 405, pp. 200–207, 2020.
- [53] Z. Ji, Y. Zhao, Y. Pang, X. Li, and J. Han, "Deep attentive video summarization with distribution consistency learning," *IEEE Trans. Neural Netw. Learn. Syst.*, vol. 32, no. 4, pp. 1765–1775, 2020.

- [54] J. Wang *et al.*, “Query twice: Dual mixture attention meta learning for video summarization,” in *Proc. 28th ACM Int. Conf. Multimed.*, New York, NY, USA, 2020, pp. 4023–4031.
- [55] E. Apostolidis, E. Adamantidou, A. I. Metsai, V. Mezaris, and I. Patras, “Video summarization using deep neural networks: A survey,” *Proc. IEEE*, vol. 109, no. 11, pp. 1838–1863, 2021.
- [56] Z. Niu, G. Zhong, and H. Yu, “A review on the attention mechanism of deep learning,” *Neurocomputing*, vol. 452, pp. 48–62, 2021.
- [57] M. Guo *et al.*, “Attention mechanisms in computer vision: A survey,” *Comput. Vis. Media.*, vol. 8, 2021.
- [58] T. Lin, Y. Wang, X. Liu, and X. Qiu, “A survey of transformers,” *AI Open*, vol. 3, pp. 111–132, 2021.
- [59] J. L. Ba *et al.*, “Layer normalization,” 2016. [Online]. Available: <https://arxiv.org/abs/1607.06450>
- [60] D. Potapov *et al.*, “Category-Specific video summarization,” in *Proc. Eur. Conf. Comput. Vis.*, 2014, pp. 540–555.
- [61] A. P. others, “Automatic differentiation in pytorch,” in *Proc. Adv. Neural Inf. Process. Syst.*, 2017, pp. 1–4.
- [62] D. P. Kingma and J. Ba, “Adam: A method for stochastic optimization,” 2014. [Online]. Available: <https://arxiv.org/abs/1412.6980>
- [63] O. Russakovsky *et al.*, “ImageNet large scale visual recognition challenge,” *Int. J. Comput. Vision*, vol. 115, pp. 211–252, 2015.